

Dynamic Analysis of a Vehicular-mounted Automatic Weapon–Planar Case

Huai-Ku Sun¹, Yun-Tien Liu¹, and Cun-Gin Chen²

¹Chung Cheng Institute of Technology, National Defense University, Ta-Hsi, Tao-Yuan, Taiwan, R.O.C.

²Ministry of National Defense, Taipei, Taiwan, R.O.C.

ABSTRACT

This study analyses the dynamic behaviour of a machine gun mounted on a four-wheeled vehicle. The entire system comprises three parts: the gun, the flexible monopod, and the vehicle. The weapon has a multi-rigid-body mechanism and comprises a rigid receiver, a rigid bolt, a bullet, a buffer, and a recoil spring. The vehicle model features a rigid vehicle body, suspension springs, shock absorbers, and wheels. The finite element method is used to model the flexible monopod connecting the gun and the vehicle. This study combines a computer-aided analysis of rigid-body mechanisms with finite element analysis of a flexible structure to derive the total equations of motion, incorporating the Lagrange multiplier. The total equations of motion are solved with numerical integration to simulate the transient response of the whole system. This approach can easily resolve the problem of rigid-flexible coupling effect, and promote the function of the whole system in the engineering design phase.

Keywords: Lagrange multiplier, finite element method, dynamic analysis, automatic weapon

NOMENCLATURE

$\underline{F}_f(t)$	Vector of the forcing functions
\underline{q}_f	Vector of nodal displacements
$\underline{g}(t)$	Vector of applied forces
$\underline{\ddot{q}}_f$	Vector of nodal accelerations
$[\mathbf{K}]$	Total stiffness matrix
\underline{q}_r	Vector of rigid body coordinates
$[\mathbf{K}]_f$	Stiffness matrix of flexible structures
$\underline{\ddot{q}}_r$	Vector of rigid body accelerations
$[\mathbf{M}]$	Total mass matrix
t	Time
$[\mathbf{M}]_f$	Mass matrix of flexible structures
$\underline{\gamma}$	Vector of quadric term of velocities
$[\mathbf{M}]_r$	Mass matrix of rigid mechanism
$\underline{\lambda}$	Vector of Lagrange multipliers
\underline{q}	Vector of total coordinates
$[\Phi]_q$	Total constraint Jacobian matrix
$\underline{\ddot{q}}$	Vector of total accelerations
$[\Phi]_{q_r}$	Constraint Jacobian matrix of rigid bodies

Superscripts

T Transpose of matrix

Subscripts

– Vector
 r Rigid
 f Flexible

1. INTRODUCTION

The ultimate objective of any weapon system is to rapidly and effectively deliver fire to the target. Increasing battlefield mobility and reducing dispersion are probably among the most effective means of achieving this goal. Dispersion can be attributed to various factors such as inherency in the weapon-ammunition combination, the forced vibration of the weapon during firing, etc. Accordingly, understanding the coupling of dynamic behaviour between the weapon, the flexible mount, and the vehicle itself becomes a crucial task for engineers during the initial design phase.

To elucidate the dynamics of a rigid-flexible coupling system, many studies¹⁻⁴ have analysed the modal characteristics of problems comprising a rigid hub and a flexible beam. Several general formulae⁵⁻⁷ have been described for the motion of a rigid body hinged to a deformable rod; for stability of motion of a rotational disk-flexible rod system, and for the 3-D motion of a rigid body during its transport. Hu⁸, *et al.* generated a computational analytical model based on the finite-element technique for determining the dynamic response of a rotating shaft on a flexible support structure with clearances. Kang⁹, *et al.* generated a modelling theory for gun systems, by assuming that the gun mechanism and its support can be simplified as two rigid bodies suspended with two springs. Bulman¹⁰ added a vehicle model into an existing gun dynamics simulation code – SIMBAD. Many analytical and numerical approaches, that elucidate mechanical systems and multibody systems have been developed since the 1980s¹¹⁻¹². Sun,¹³⁻¹⁵ *et al.* studied the dynamic behaviours

of a machine gun mechanism mounted on a flexible tripod for planar and spatial cases, and combined it with the exterior ballistics to forecast the firing precision, accuracy, and dispersion of that system.

This study analyses the dynamic behaviour of a machine gun mounted on a four-wheeled vehicle via a flexible monopod. The weapon itself and the vehicle suspension system are modelled as multi-rigid-body systems, and the finite element method is used to model the monopod. Detailed equations of motion are developed. The resulting equations, which comprise two kinds of equations of motion-multi-rigid-body and finite element dynamics,-are then integrated numerically.

2. EQUATIONS OF MOTION

2.1 Multi-rigid-body Mechanisms

Planar dynamic analysis adopts equations of motion for the constrained multi-rigid-body system and acceleration equations¹¹. It can be written as

$$\begin{bmatrix} [M]_r & [\Phi]_{q_r}^T \\ [\Phi]_{q_r} & [0] \end{bmatrix} \begin{Bmatrix} \ddot{q}_r \\ -\underline{\lambda} \end{Bmatrix} = \begin{Bmatrix} \underline{g}(t) \\ \underline{\gamma} \end{Bmatrix} \quad (1)$$

where the mass matrix of rigid bodies $[M]_r$ denotes a diagonal nonsingular matrix; the constraint Jacobian matrix $[\Phi]_{q_r}$ denotes a function of q_r ; $\underline{g}(t)$ encompasses the vectors of applied forces and moments that act on all bodies in the system.

2.2 Flexible Structure

The finite element method is currently a significant tool in analysis and design, and is commonly adopted by engineers. This study adopts the following equations of motion for flexible structures¹⁵

$$[M]_f \ddot{q}_f + [K]_f q_f = F_f(t) \quad (2)$$

2.3 Multi-rigid-body Mechanisms Mounted on Flexible Structures

Since the analyses for rigid-body mechanisms and the finite element method are based on completely different assumptions, these produce different equations of motion. Hence, an innovative method is required to combine these into one equation to solve it numerically.

An extra rigid joint besides the kinematic joints existing in the gun mechanism is considered. The gun mechanism is assumed to be mounted rigidly on the top of a flexible monopod, and the bottom of that is connected rigidly to the vehicle. The physical constraints provided by the rigid joint are that the displacement and rotation vectors of the connecting point on the mechanism and on the monopod always remain the same. The resulting constraint equations and the associated Jacobian matrix can be efficiently derived. Finally, after considering the rigid joint as an extra constraint, the Eqns (1) and (2) can be combined to yield.

$$\begin{bmatrix} [M] & [\Phi]_{q_r}^T \\ [\Phi]_{q_r} & [0] \end{bmatrix} \begin{Bmatrix} \ddot{q} \\ -\underline{\lambda} \end{Bmatrix} = \begin{Bmatrix} \underline{g}(t) \\ \underline{\gamma} \end{Bmatrix} - \begin{bmatrix} [K] & [0] \\ [0] & [0] \end{bmatrix} \begin{Bmatrix} q \\ 0 \end{Bmatrix} \quad (3)$$

where the mass matrix $[M] = \begin{bmatrix} [M]_r & [0] \\ [0] & [M]_f \end{bmatrix}$ has both of the mass matrices for multi-rigid-body mechanisms and flexible structures $[\Phi]_{q_r}$ denotes the constraint Jacobian matrix incorporating all of the kinematic constraints associated with multi-rigid-body mechanisms and the rigid joint; $\underline{g}(t)$ denotes the vectors of applied forces that act on all rigid components and the flexible structure in the system; $[K] = \begin{bmatrix} [0] & [0] \\ [0] & [K]_f \end{bmatrix}$

denotes the stiffness matrix; $q = \begin{Bmatrix} q_r \\ q_f \end{Bmatrix}$ and $\ddot{q} = \begin{Bmatrix} \ddot{q}_r \\ \ddot{q}_f \end{Bmatrix}$ denote the vectors of coordinates and acceleration, respectively.

3. NUMERICAL EXAMPLE

3.1 Gun System Model

The gun model employed in this work was proposed by Sun,^{13 et al.} It simulates the motion of gun components, the deformation of the flexible monopod and the coupling effect between these in various firing situations. Following simplification, the gun model is composed of a buffer spring, a recoil spring, a receiver, a bolt, a bullet and a flexible monopod; the monopod is divided into two frame elements. Figure 1 shows a diagram of the gun model system.

3.2 Vehicle System Model

The vehicle model employed here was similar to that addressed by Bulman¹⁰. It comprised four suspensions and four tyres. The suspension was considered to have linear spring stiffness and damping. Each wheel was represented as a lumped mass with linear tire stiffness. The gun system was mounted onto the vehicle via a rigid joint in a 2-D plane, as illustrated in Figure 2. The vehicle is considered not to be traveling during firing, meaning that no variation of road force was applied.

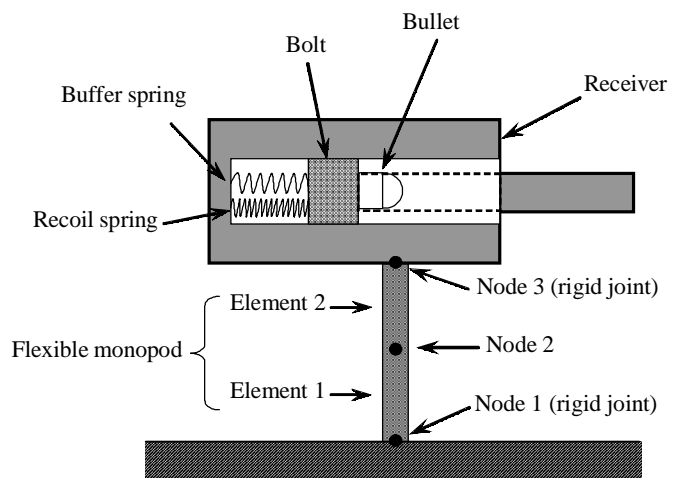


Figure 1. 2-D model of machine gun system.

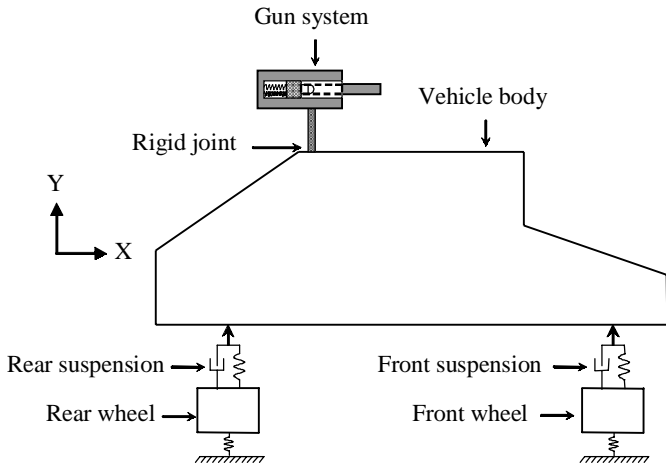


Figure 2. 2-D model of four-wheeled vehicle.

Table 1 shows the configuration and degrees of freedom(DOFs) of the entire system. The system has seven rigid bodies, two translational joints, and one composite joint: One translational joint linked the bolt and receiver, while the other linked the bullet and receiver. The composite joint linked the bullet and bolt. Tables 2 and 3 list the inertia properties and other parameters of the complete

system. A FORTRAN program was developed to perform planar dynamic analysis of this case.

3.3 Firing Sequence

The firing duration for each round was very short. For each round, the firing sequence could be split into four continuous stages.

- At the beginning of the first stage, the bolt was pulled back to the in-battery position, and the recoil spring was compressed. The bolt was then released and moved forward. The first stage was completed when the bolt arrives at the firing position.
- At the beginning of the second stage, the ammunition was fired, and the bullet was propelled to move forward rapidly by the chamber pressure. The bolt decelerated to stop, then moved backwards.
- The second stage was completed once the bullet left the muzzle. The bolt continued moving backwards during the third stage, until it compressed the buffer spring.
- In the fourth stage, the bolt continued to move back under the action of not only the recoil spring but also a much stiffer buffer spring to stop. The bolt then started to be pushed back to its in-battery position.

Table 1. Configuration and degree of Freedom of entire system

Gun system	Mechanism configuration				Number of nodes in monopod	DoF
	Number of rigid body	Constrained joint				
		Number of translation joint	Number of composite joint*	Number of rigid joint		
With mount only	3	2	1	1	3	18
With mount and vehicle	7**	2	1	2	3	30

* Composite joint is called the revolute-translational joint.

** Including ground body.

Table 2. Inertia properties of the rigid-body mechanisms

Body	Mass (kg)	Polar moment of inertia (kg-m ³)	
Receiver	4	0.004.	
Bolt	1.2	0.0012	
Bullet	0.24	0.0005	
Vehicle	2,400	3,600	
Rear Wheel	50	8.0	
Front Wheel	50	8.0	
	Spring free length (m)	Spring constant (Nt/m)	Damping ratio (Nt.s/m)
Buffer Spring	0.5	400	50
Recoil Spring	1	100	i ∅
Rear Suspension	0.2246	480,000	24,000
Front Suspension	0.2246	480,000	24,000
Rear Wheel Elasticity	0.1286	420,000	i ∅
Front Wheel Elasticity	0.1286	420,000	i ∅

4. RESULTS AND DISCUSSION

4.1 Single-round Firing Condition

The firing angle was set to 0° in this study, but it can be set to any angle for various simulation needs. The propellant force was assumed to be 2000 Nt. The 2-D frame element is utilised to model the flexible monopod. Numerical integration was performed with the fourth-order Runge-Kutta algorithm. Since the cyclic time of shoot was short, the numerical integration time step needed to be very small to get detailed information. This study tried various time steps from $1.0E-3$ s to $1.0E-5$ s. When the time step was $> 1.0E-4$ s, the truncation error would be accumulated and caused the kinematic constraints to be violated and yielded incorrect results. Figure 3 presents the velocity-time curve of the bolt for different time steps. The velocity of bolt was stable when the time step was 1.0×10^{-5} s or 5.0×10^{-5} s, but not when time step was 1.0×10^{-4} s.

The integration time step was then set to be 1.0×10^{-5} s. The simulation results shows that the cyclic time for a single shot was 0.1353 s where the first stage took 0.1003 s; the second stage took 0.0092 s; the third stage took 0.0228 s, and the fourth stage took 0.0030 s.

Figure 4 shows the velocity-time curve of the bolt. The curve presents different curvatures in the x-direction at every stage, due to different forcing conditions acting on the bolt. Only the recoil spring force pushes the bolt forward in the first stage. In the second stage, the chamber pressure pushes the bolt backwards, but the recoil spring still pushes on the opposite direction. Only the recoil spring pushes the bolt in the third stage. Both recoil and buffer springs pushes the bolt in the fourth stage. Figure 5 depicts the trajectory of the bolt in each stage of single firing.

Figure 6 presents the displacement-time cure of the receiver. Significantly, the receiver moves fastest in the fourth stage. This finding would be expected, since the recoil spring and buffer spring pushes the receiver simultaneously in the fourth stage, while only the recoil spring pushes the receiver in the stages one to three. Figure 7 shows the trajectory of the receiver. At the end of shot, the receiver reaches a position with downward and rearward displacements from its initial position, matching the recoil motion felt by gunner.

Since the receiver and the barrel are considered as a single body, the rotation angle of the receiver is the firing angle of the gun in this case. This angle dominates the accuracy and precision of firing. Figure 8 plots the rotation angle of the receiver of gun, node 3 of the monopod (i.e. rigid joint), and the vehicle body. The receiver and rigid joint are clearly consistent with each other, demonstrating that the constraint equation has been applied correctly in the developed program. This graph also shows the vehicle pitch, which is a smoother curve, revealing that the receiver angle continues to follow the vehicle pitch from first to fourth stages. Because the bullet leaves the muzzle at the end of second stage, the vehicle pitch has a significant impact on the accuracy of the gun.

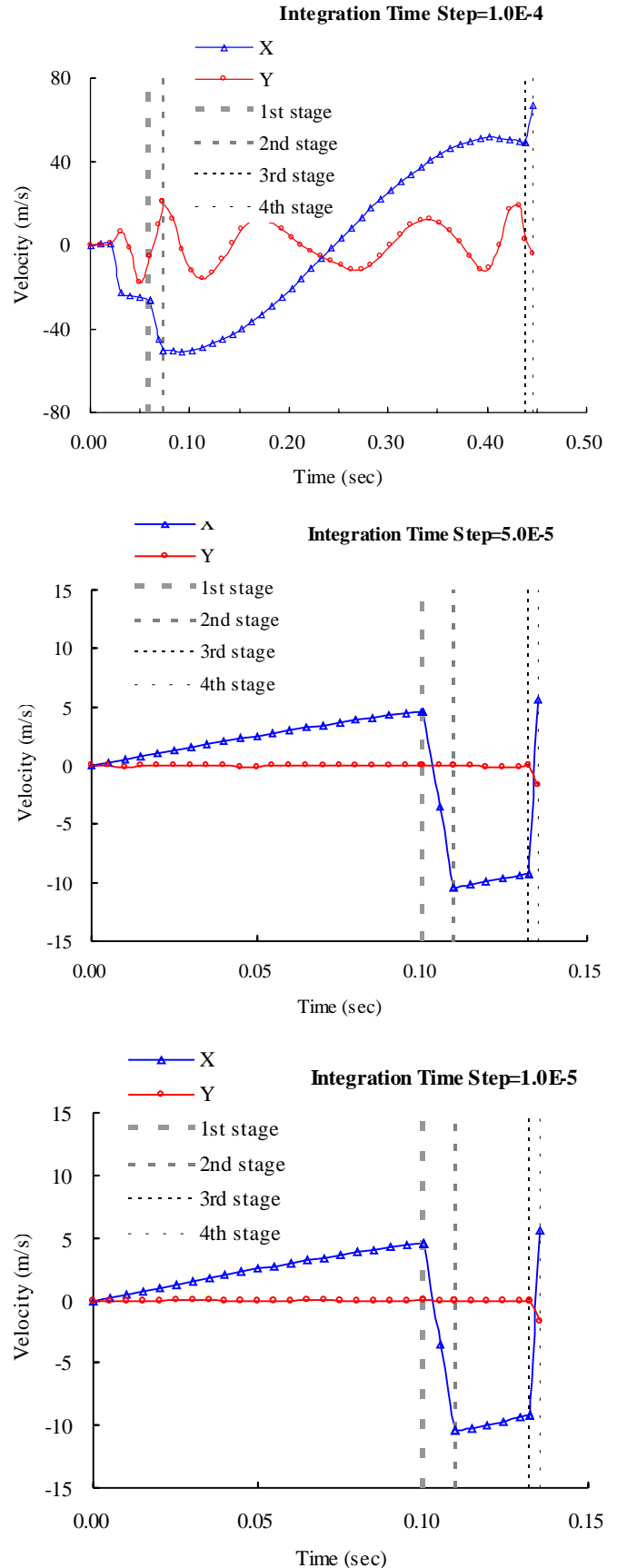


Figure 3. Velocity-time diagram of the bolt using various time steps in single-round firing.

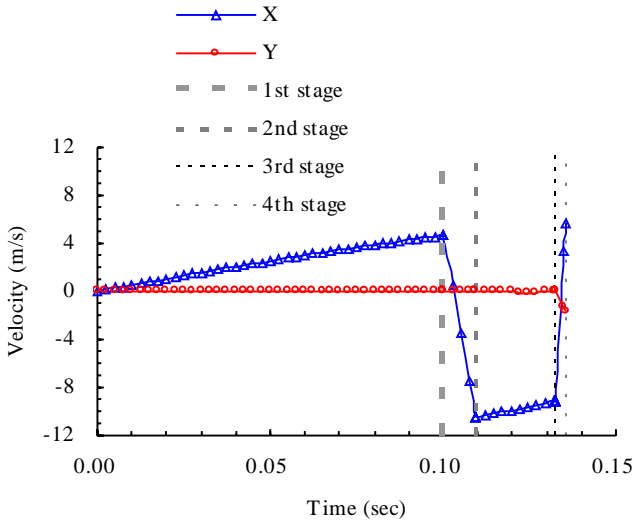


Figure 4. Velocity-time diagram of the bolt in single-round firing condition.

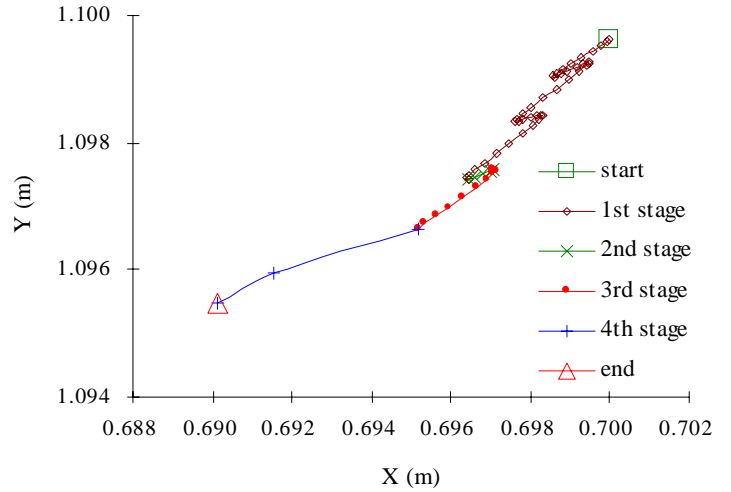


Figure 7. Trajectory of the receiver in single-round firing condition.

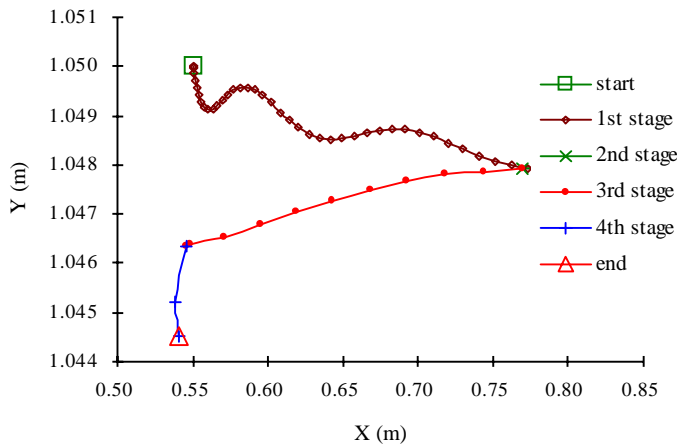


Figure 5. Trajectory of the bolt in single-round firing condition.

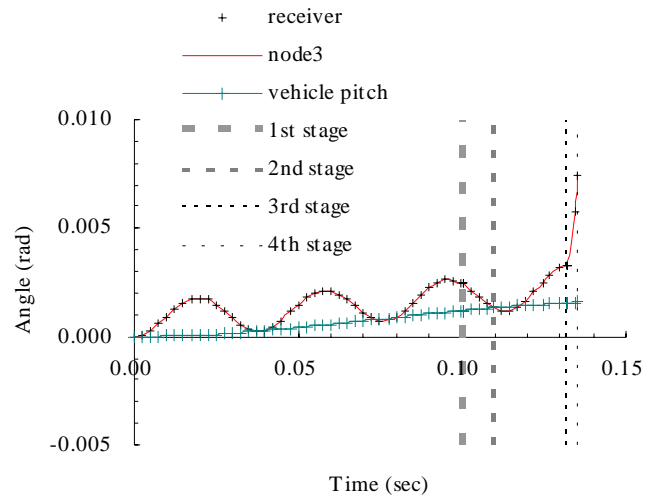


Figure 8. The rotation angle-time diagram in single-round firing condition.

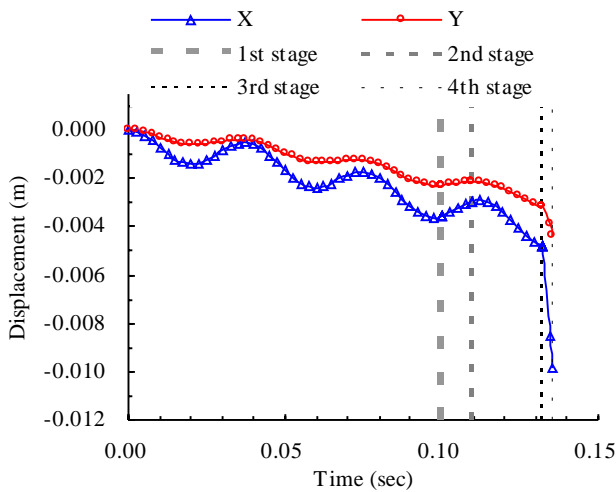


Figure 6. Displacement-time diagram of the receiver in single-round firing condition.

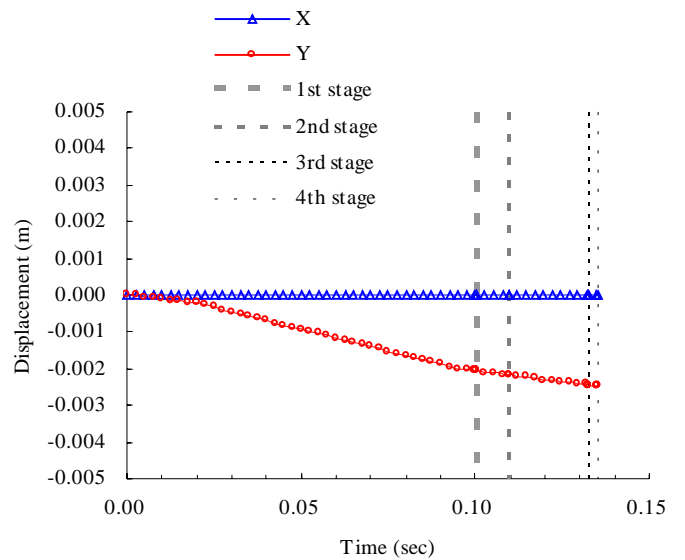


Figure 9. Displacement-time diagram of rear wheel in single-round firing condition.

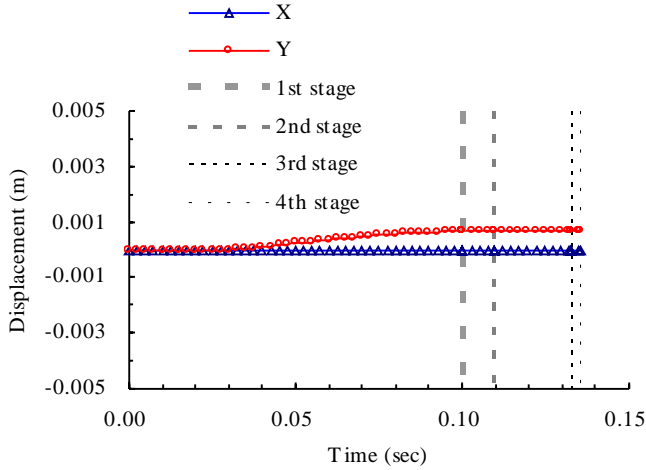


Figure 10. Displacement-time diagram of front wheel in single-round firing condition.

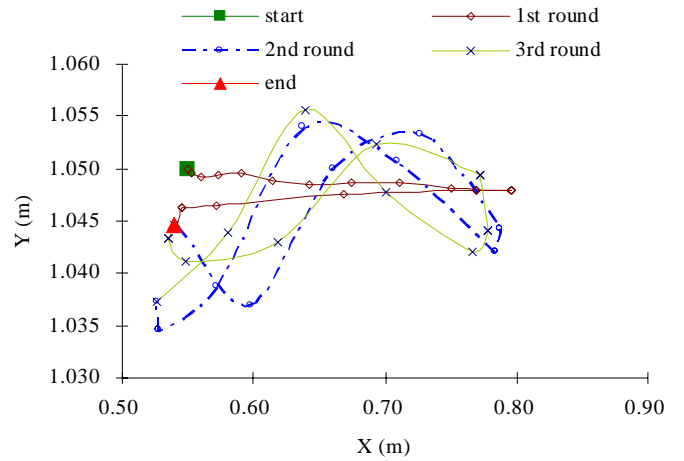


Figure 13. Trajectory of the bolt in 3-round burst firing condition.

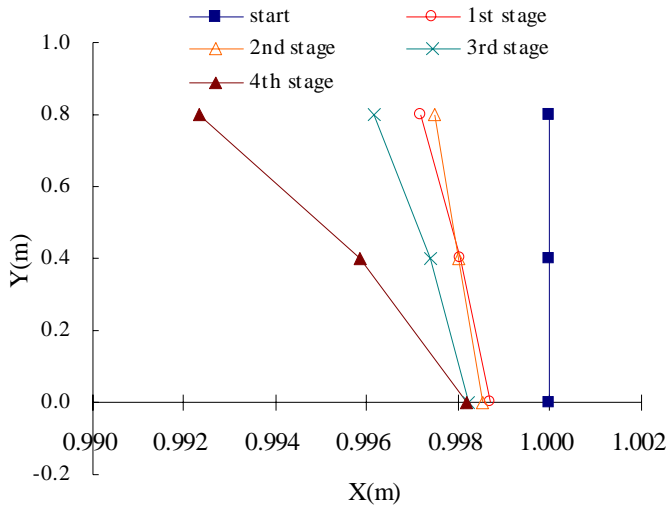


Figure 11. Nodal displacement of monopod in single-round firing condition.

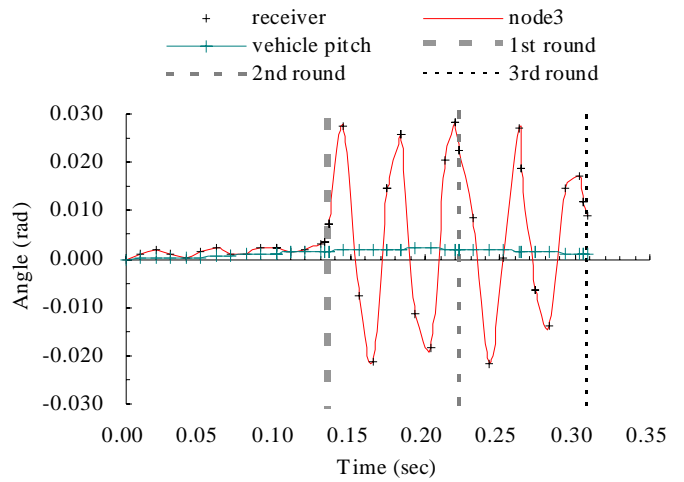


Figure 14. The rotation angle-time diagram in 3-round burst firing condition.

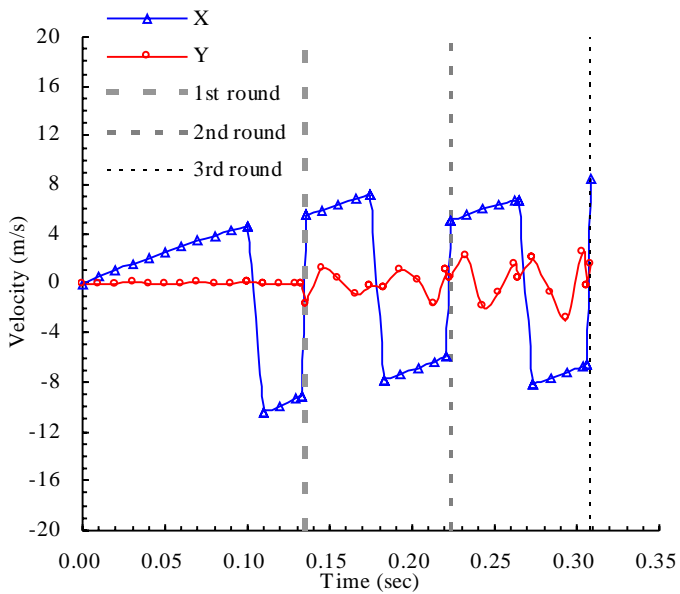


Figure 12. Velocity-time diagram of the bolt in 3-round burst firing condition.

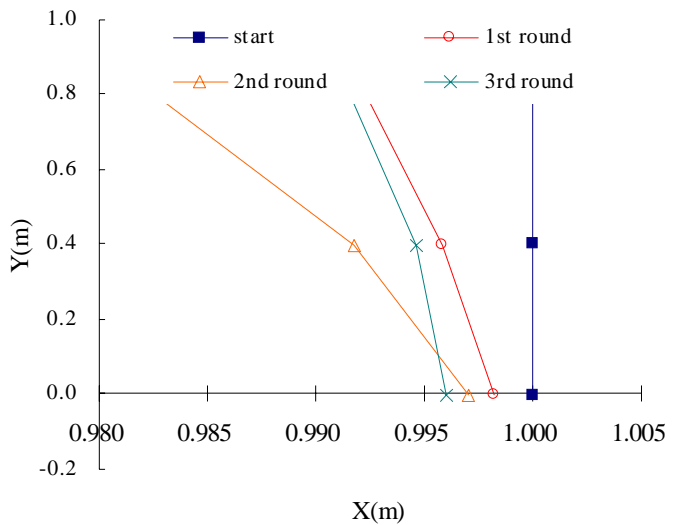


Figure 15. Nodal displacement of monopod in 3-round burst firing.

Table 3. Material properties and dimension of the flexible monopod

Material Properties	Mass density and modulus		
	ρ (kg/m ³)	E (pa)	-
	7900	2.0E11	-
Dimension	Length (m)	Cross Section (m ²)	Moment of Inertia (m ⁴)
	0.8	0.0004	3.0E-7

Table 4. Maximum pitch angle of the receiver at each round of 3-round burst firing

Gun system	1st round (rad)	2nd round (rad)	3rd round (rad)
With monopod only	0.0019	0.0260	0.0171
With monopod and vehicle	0.0033	0.0283	0.0224

Figures 9 and 10 present the displacement-time curves of the rear wheel and front wheel, respectively. The rear wheel moves downwards, while the front wheel moves upwards simultaneously. This behaviour is also consistent with the direction of vehicle pitch in Figure 8. The coupling between the rigid gun mechanism and the flexible monopod causes the monopod to move and deform under the recoil force. Figure 11 shows the resulting nodal displacements.

4.2 Three-round Burst Firing Condition

The initial conditions were the same as those associated with firing a single-round. The cyclic time for third round burst firing was 0.3086 s as shown in the simulation. The first round took 0.1353s; the second round took 0.0873s, while the third round took 0.0860 seconds. Notably, the coupling effect becomes strong, since the vibration caused by previous round influences the next round in the three-round burst condition. Figures 12 and 13 reveal the velocity-time curve and the bolt trajectory in three-round burst firing.

Figures 14 and 15 display the dynamic response of the receiver and the flexible monopod in three round burst firing. Comparison with the single-round result reveals that the behaviours of the second and third round become much violent. Table 4 lists the maximum pitch angle of the receiver at each round. According to this table, the system with mount and vehicle has a much greater pitch angle than the system with mount only, signifying that both the mount and vehicle influence the vibration of the receiver. The performance of machine gun is strongly affected by variations of weapon support.

5. CONCLUSION

This study elucidates the dynamic behaviour of a gun mounted on a vehicle in single-round and three-round burst firing, and indicates that the motion of the vehicle and monopod influence on the gun vibration significantly. A systematical approach to formulate the dynamic response of a gun mechanism mounted on a four wheeled vehicle by combining the rigid-body dynamic with the finite element

method, and by introducing the rigid joint, is developed successfully. The interaction between rigid mechanisms and flexible monopod can be monitored to predict and analyse the performance of the overall system. This approach allows the system's parameters to be varied to optimise the performance of the weapon system. The coupling effect can be treated effectively. A feature work may examine a similar system but in a 3-D analysis.

REFERENCES

1. Cai, G.P. & Hong, J.Z. Study on two dynamic models for a rigid-flexible coupling system. *Acta Aeronaut. et Astronaut. Sinica*, 2004, **25**(3), 248-53.
2. Yang, H.; Hong, J.Z. & Yu, Z.Y. Vibration analysis and experiment investigation for a typical rigid-flexible coupling system. *Journal of Astronautics*, 2003, **23**(2), 67-72.
3. Yang, H.; Hong, J.Z. & Yu, Z.Y. Study on two dynamic models for a rigid-flexible coupling system. *J. Shanghai Jiaotong Univ.*, 2002, **36**(11), 1591-595.
4. Hu, Z.D. & Hong, J.Z. Modeling and analysis of a coupled rigid-flexible system. *Appl. Math. Mech.*, 1999, **20**(10), 1167-174.
5. Kayuk, Y.F. & Pyatov, A.L. Motion of a rigid body hinged to a deformable rod. *Sov. Appl. Mech.*, 1990, **25**(11), 1139-146.
6. Kayuk, Y.F. & Tverdokhlebl, Y.V. Three-dimensional motions of a rigid body during its transport. *Sov. Appl. Mech.*, 1987, **23**(10), 936-43.
7. Kayuk, Y.F. Stability of motion of a rotating disk-flexible rod system. *Sov. Appl. Mech.*, 1989, **25**(2), 201-08.
8. Hu, K., Mourelatos, Z.P. & Vlahopoulos, N. Computational analysis for dynamic response of a rotating shaft on flexible support structure with clearances. *J. Sound Vib.*, 2003, **267**, 1-28.
9. Kang, X.Z.; Ma, C.M. & Wei, X.D. Modeling theory of gun system. Defense Industry Publishing Co, Beijing, 2003.
10. Bulman, D.N., The effects of vehicle and barrel motion

on the accuracy of a repeat fire small cannon. *In Proceedings of the Eighth U.S. Army Symposium on Gun Dynamics*, Newport, Rhode Island, 14-16 May 1996. pp.1-1-1-12.

11. Nikravesh, P.E. Computer-aided analysis of mechanical systems. Prentice-Hall, Inc, New Jersey, 1988.
12. Shabana, A.A. Dynamics of multibody systems. John Wiley & Sons, New York, 1989.
13. Sun, H.K., Chen, C.G., and Shen, Y.C. Dynamic analysis of rigid-body mechanisms mounted on flexible support structures—planar case. *J. Mater. Sci. Forum*, 2006, **505-507**, 589-94.
14. Sun, H.K.; Chen, C.G.& Shen, Y.C. Numerical simulation of firing precision of automatic weapon systems. *J.Chung Cheng Inst. Technol.*, 2006, **34(2)**, 223-32.
15. Sun, H.K., Chen, C.G.& Wang, H.P. Dynamic analysis of rigid-body mechanisms mounted on flexible support structures—spatial case. *J.Chinese Soci. Mech. Engs.*, 2007, **28(6)**, 585-91.
16. Yang, T.Y. Finite element structural analysis. Prentice-Hall, Inc., New Jersey, 1986.

Contributors



as an Associate Professor. His research interests are weapon system engineering, ballistics and CAA of mechanical systems.

Colonel (Ret.) Huai-Ku Sun received his PhD. degree from the North Carolina State University, U.S.A. in 1991. Before his retirement from military service in 2008, he was the Deputy Executive Director of the National Defense University, Taiwan, R.O.C. At present, he serves in the Department of Power Vehicle and System Engineering of the Chung Cheng Institute of Technology, National Defense University



Colonel Yun-Tien Liu received his Master's degree from the Department of Military Engineering, Chung-Cheng Institute of Technology, R.O.C. in 1993, and is presently a PhD student in the Chung-Cheng Institute of Technology, National Defense University. His dissertation research is focused on the weapon system dynamics.